Superinfection Exclusion of Alphaherpesviruses Interferes with Virion Trafficking

James P. Cwick,[a] Jonathan E. Owen,[a] Irina Kochetkova,[a] Kyle S. Hain,[a] Nick Van Horssen,[a] Matthew P. Taylor[a]

[a]Department of Microbiology & Cell Biology, Montana State University, Bozeman, Montana, USA

ABSTRACT Superinfection exclusion (SIE) is a phenomenon in which a primary viral infection interferes with secondary viral infections within that same cell. Although SIE has been observed across many viruses, it has remained relatively understudied. A recently characterized glycoprotein D (gD)-independent SIE of alphaherpesviruses presents a novel mechanism of coinfection restriction for herpes simplex virus 1 (HSV-1) and pseudorabies virus (PRV). In this study, we evaluated the role of multiplicity of infection (MOI), receptor expression, and trafficking of virions to gain greater insight into potential mechanisms of alphaherpesvirus SIE. We observed that high-MOI secondary viral infections were able to overcome SIE in a manner that was independent of receptor availability. We next assessed virion localization during SIE through live microscopy of fluorescently labeled virions and capsid assemblies. Analysis of these fluorescent assemblies identified changes in the distribution of capsids during SIE. These results indicate that SIE during PRV infection inhibits viral entry or fusion while HSV-1 SIE inhibits infection through a postentry mechanism. Although the timing and phenotype of SIE are similar between alphaherpesviruses, the related viruses implement different mechanisms to restrict coinfection.

IMPORTANCE Most viruses utilize a form of superinfection exclusion to conserve resources and control population dynamics. gD-dependent superinfection exclusion in alphaherpesviruses is well documented. However, the undercharacterized gD-independent SIE provides new insight into how alphaherpesviruses limit sequential infection. The observations described here demonstrate that gD-independent SIE differs between PRV and HSV-1. Comparing these differences provides new insights into the underlying mechanisms of SIE implemented by two related viruses.

KEYWORDS alphaherpesvirus, pseudorabies virus, herpes simplex virus type 1, superinfection exclusion, fluorescent protein, herpes simplex virus, virus entry

Alphaherpesviruses are a family of neurotropic viruses with the ability to establish latency in neurons and have a broad impact on human health and agriculture. Herpes simplex virus 1 (HSV-1) has achieved a global infection rate of 80%, with approximately 40% of individuals seropositive within the United States (1, 2). Documented cases of both symptomatic and asymptomatic shedding within infected individuals promote high circulating populations of HSV and the increased probability for sequential exposure (3–5). These conditions of viral prevalence and transmission increase the probability of superinfection within an individual that can lead to the development of recombinant genomes with novel phenotypes (6–8). These novel recombinant genomes can present with various degrees of virulence depending upon a wide range of factors. Recombinant viruses generated from superinfection have been observed in many alphaherpesviruses, including varicella-zoster virus (VZV) and herpes simplex virus 1 and 2 (9–14). Pseudorabies virus (PRV) is an alphaherpesvirus of pigs that greatly affects agricultural practices and production. An estimated $500 million is spent annually in the United States for vaccination, disease surveillance, and livestock eradication (11). The prevalent use of glycoprotein-E-negative vaccines has allowed possible recombination with circulating strains of PRV (15). Despite concerns about novel recombinant

genomes, we still do not know much about the mechanisms that HSV-1 and PRV employ to either limit coinfection or interfere with superinfecting virions.

Superinfection exclusion (SIE) is a process by which an infecting virus prevents subsequent infection of the same cell. Typically, SIE occurs only between identical or closely related viruses, a characteristic that distinguishes this virally mediated process from cellular antiviral responses. First discovered for tobacco mosaic virus in the 1920s, SIE has been utilized by plant virologists to generate "cross-protection" in crops, whereby inoculation with a mildly pathogenic virus can exclude disease-causing strains (16, 17). Interest in mammalian SIE picked up in the 1970s, when it was discovered that the endogenous proviral mouse gene FV1 (genetically comparable to the retrovirus gag gene) was able to confer resistance to various strains of murine leukemia virus (18). SIE has since been observed for several viral species, all of which employ unique mechanisms for inhibiting different aspects of secondary virus infection. For example, influenza and HIV prevent the attachment and entry of secondary virions by occluding, internalizing, or downregulating cellular coreceptors (19–21). In certain persistent viral infections, like duck hepatitis B virus and bornaviruses, the stoichiometry of late-stage viral replication elements generates unfavorable conditions for incoming viruses, preventing the transcription of secondary virus genes (22). The mechanism of SIE also influences the timing of exclusion, which can have important implications on both its pathological and therapeutic relevance. Such is the case for alphaherpesviruses, which employ mechanistically independent early and late forms of SIE (23).

Research into SIE for alphaherpesviruses has focused on the role and effect of glycoprotein D (gD) expression (24, 25). However, another mechanism for alphaherpesvirus SIE has been observed that is independent of gD expression (23). This gD-independent SIE is potentially a departure from the canonical mechanism of occlusion or internalization of cellular receptor proteins like nectin-1 (26, 27). Additionally, gD-independent SIE was dependent upon active viral replication and protein synthesis during the first 2 h of primary viral infection to exclude secondary viral inoculum. However, these results could isolate neither the step of viral infection inhibited nor the mechanism contributing to gD-independent SIE (23). To better characterize and understand SIE for both HSV-1 and PRV, we applied a combination of live fluorescence microscopy with fluorescent protein-expressing recombinant viruses to understand inhibition of secondary infection. We investigated the roles of multiplicity of infection (MOI), receptor internalization, and virion distribution to understand PRV and HSV-1 SIE. Together, results from this work will demonstrate that SIE interferes with early steps of viral infection to suppress the replication of superinfecting viruses.

RESULTS

PRV SIE is dependent upon MOI. SIE is a virally induced process that can directly or indirectly inhibit or block secondary virion infection (28). However, the timing and extent of SIE for any virus are dependent on several variables of infection, including the inoculating dose. The number of virions infecting a single cell, the multiplicity of infection (MOI), has an immense effect on outcomes of viral replication. In previously published data, we established the timing of HSV-1 and PRV SIE under equivalent inoculation conditions of MOI 10. We hypothesized that SIE established by the initial MOI of the primary virus might be overcome with various MOIs of the secondary virus.

To test the effect of MOI on SIE, we evaluated the effect of different doses for the primary and secondary inoculations. For all infections, application of the secondary viral inoculum occurred 2 h after removal of the primary inoculum. To detect infection by both primary and secondary viruses, we evaluated fluorescent protein expression from recombinant viruses. Fluorescent protein expression correlating with either primary (cyan fluorescent protein [CFP]) or secondary (yellow fluorescent protein [YFP]) infection was evaluated by fluorescence microscopy at 7 to 9 h postinoculation (Fig. 1A). The extent of primary infection is determined by CFP expression, with representative images of CFP expression at each MOI for the given row. Secondary infection was determined by the extent of YFP expression, with representative images shown across different MOIs. The extent of YFP expression inversely reflects the degree of SIE. Fewer YFP-positive nuclei indicate greater SIE, while more YFP-positive nuclei indicate
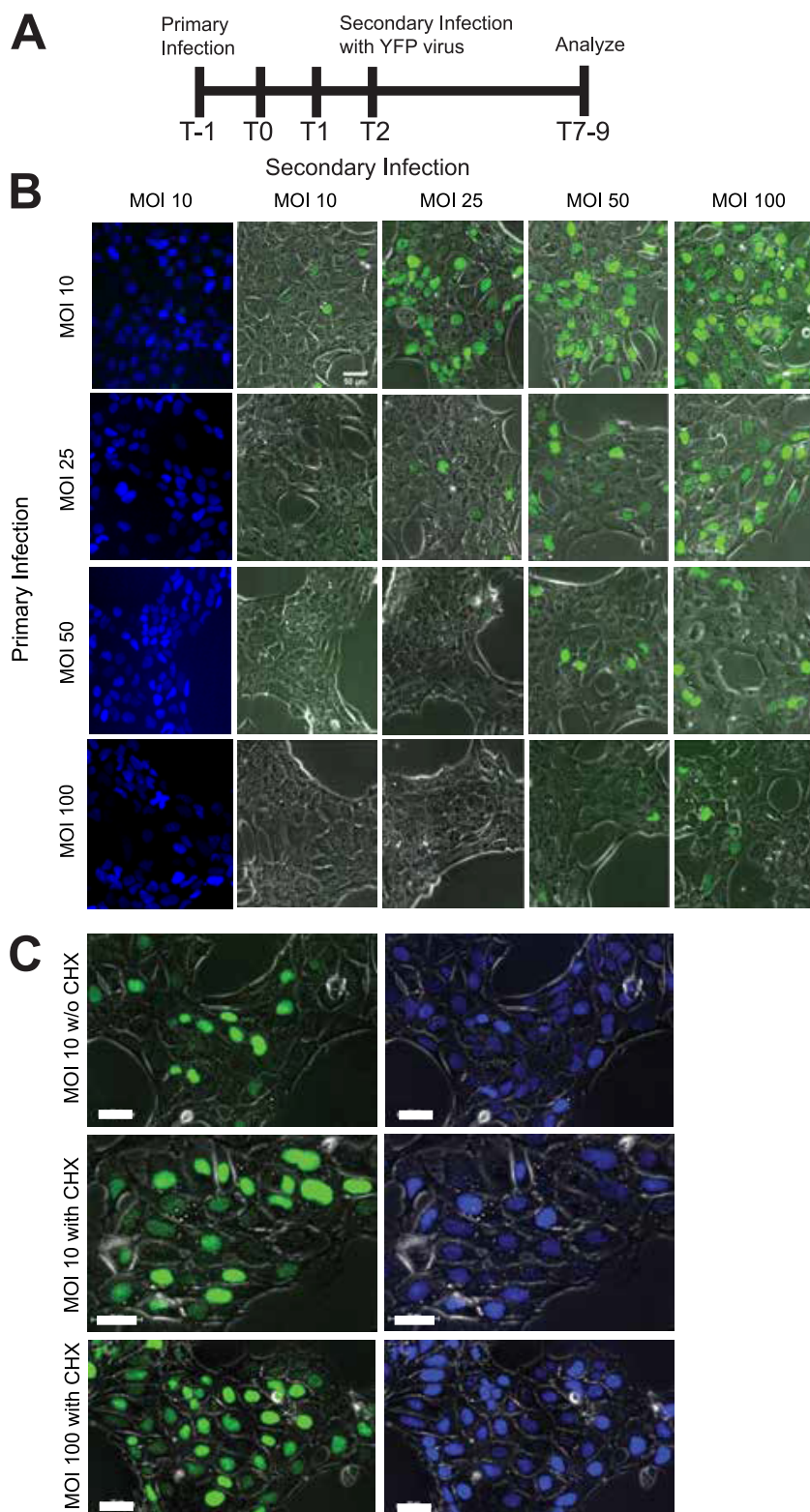
FIG 1 SIE dependence on primary and secondary MOIs. Experiments done in triplicate on PK15 cells. (A) Diagram of the timeline of experimentation. (B) Comparison of SIE across a 4 BY 4 matrix of primary and secondary infections. The top row corresponds to the MOI of the secondary virus (YFP labeled), while the vertical column corresponds to the MOI of the primary virus. Images were acquired and analyzed 7 to 9 h after initial infection (or 4 to 6 h after superinfection). Column with CFP fluorescent expression represents confluent infection with primary virus and is representative of

less SIE. In line with our previous report, we observe extensive SIE when primary and secondary inoculations are an equal MOI (Fig. 1B). Conditions where the secondary MOI was lower than the initial infection resulted in reduced YFP-positive nuclei, indicative of greater or more effective SIE. In line with our hypothesis, higher MOIs for the secondary inoculation were able to overcome SIE, resulting in greater numbers of YFP-expressing cells. The greatest difference of YFP expression occurred with a low primary inoculation and a high secondary MOI (MOI: 10 primary, 100 secondary). The extent of fluorescent protein (FP) expression under these conditions was nearly equivalent to that observed with simultaneous inoculation of the two viruses, suggesting no exclusion of the secondary virus.

In previous work, it was observed that alphaherpesvirus SIE could be disrupted using the protein synthesis inhibitor cycloheximide (CHX) (23). To determine if protein synthesis is necessary for SIE at the different inoculating doses, we utilized CHX treatment to alleviate SIE at the extremes of our inoculating doses of MOI 10 and 100. Fluorescent protein detection during SIE was repeated with CHX treatment during the 2-h window between primary and secondary inoculation. CHX treatment during both MOI 10 and 100 infections alleviated SIE, with an increase of YFP-expressing cells (Fig. 1C). Importantly, there are relatively similar extents of YFP-positive nuclei at both conditions, consistent with a similar mechanism of exclusion independent of MOI.

The data support that PRV SIE is dependent upon MOI of both the primary and secondary viruses. Alleviation of SIE occurred either by an overwhelming inoculating dose of secondary virus or through inhibition of protein synthesis by CHX treatment. In both cases, protein production by either cellular or viral origins still plays an important role in the dynamics contributing to SIE establishment.

SIE is independent of surface receptor modulation. Since other forms of SIE disrupt receptor-mediated entry of virions, a possible explanation for SIE disruption of alphaherpesviruses could be dependent upon modulation of available surface receptors. In fact, alphaherpesviruses like HSV-1 have shown cell-dependent entry mechanisms of both direct fusion with the cell membrane and low pH endocytic processes that later release virions (29). In both cases, cell entry is mediated primarily by gD engagement with cellular receptors: herpes virus entry mediator (HVEM), nectin-1 and nectin-2, and heparan sulfate (30). During infection, modulation of receptor availability occurs through internalization of surface expression for cellular entry receptors like nectin-1 (31, 32). A decrease in the availability of cellular receptors following primary infection would thus decrease the capacity for secondary virion entry. We hypothesized that reduction of cellular receptors on the surface of cells could mediate SIE.

To address this hypothesis, nectin-1 surface expression was evaluated during PRV infection. We chose nectin-1 as a model receptor due to the ubiquity of cellular expression and its use by multiple alphaherpesvirus. PK15 cells were either mock-infected or infected with wild-type PRV. Following infection, cells were then either mock treated or treated with CHX. At the indicated times postinfection, cells were fixed, stained, and assessed by flow cytometry for surface-expressed nectin-1.

For these experiments, changes in surface nectin-1 detection were compared at 0, 1, and 2 h post-inoculum removal during the time of SIE induction. At 0 h post-inoculum removal (T_0), there was a significant drop in the surface of nectin-1 expression during PRV infection. This outcome supports past literature that observable internalization of nectin-1 occurs following alphaherpesvirus infection (33). However, T_1 observes no notable difference regarding surface expression of nectin-1 for PRV infection with or without CHX treatment (Fig. 2). Overall, the data demonstrate that relative expression of nectin-1 for CHX-treated and -untreated conditions remains the same. Although CHX inhibits SIE, it does reduce surface nectin-1 levels. This supports a model that reduced nectin-1 expression following

FIG 1 Legend (Continued)

all conditions in the row. (C) Analysis of SIE with CHX treatment. Experiments were repeated with previously described SIE conditions. CHX treatment occurred between the application of the primary and secondary inocula. The top row depicts fluorescent protein expression without CHX (MOI 10), while the middle (MOI 10) and the bottom (MOI 100) depict fluorescent protein expression with CHX treatment.

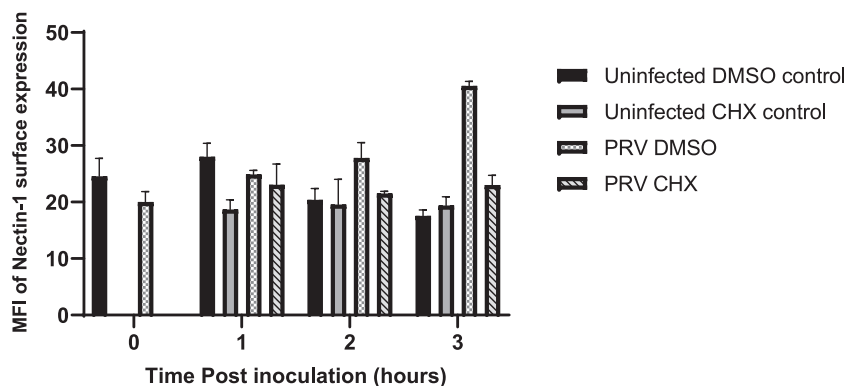## Nectin Surface Expression during PRV infection

FIG 2 Cell surface nectin expression does not correlate with SIE during PRV infection. Depicted is the percentage of nectin-1 expression on the surface of the PK15 cells during PRV infection (MOI 50) at hours after inoculum removal. CHX treatment occurred 1 h before the application of infection, and CHX was then removed. Cells were gated for being positive of stained fluorescence compared to unstained controls.

primary virion entry is still sufficient for effective entry of a secondary virus. These results surmise that any potential SIE mechanism is not mediated by changes in nectin-1 surface expression.

SIE affects entry of secondary virions. Our previous experiments using fluorescent viruses indicate that glycoprotein D-independent SIE interferes with secondary viral infection. However, they could not isolate the step(s) of infection that were inhibited (23). Inhibition of one or several steps of infection—including attachment, entry, capsid trafficking, or transcription—could result in inhibition of secondary virus-associated FP expression (34, 35). To understand the extent of secondary virion inhibition during SIE, we developed a method to monitor virion entry and trafficking using direct FP fusions to virion components.

To determine how SIE affects early steps of viral entry, time-lapse microscopy was performed with a dual fluorescently labeled virion (PRV 137). As modeled in Fig. 3A, PRV137 produces virions that incorporate a green fluorescent protein (GFP) fusion to viral protein gM and a monomeric red fluorescent protein (mRFP) fusion to the capsid-associated protein VP26 (31). Colocalization of both fluorophores indicates an intact virion, while dissociation of the two fluorescent signals occurs following entry of the capsid into the cell. The gM protein should remain at the plasma membrane, while the VP26 viral capsid protein will traffic toward the nucleus for insertion of the viral genome and subsequent viral replication. Microscopic examination of secreted PRV 137 virions used for experimental inoculation observed that approximately 75% of fluorescent capsid assemblies (red puncta) contain detectable amounts of GFP (Fig. 3B). Therefore, these colabeled virions provide an excellent means to evaluate the distribution and structure of virions during entry.

To evaluate virion entry under SIE conditions, sequential micrographs of cells were acquired using a live-imaging approach after inoculation (36). For our live-imaging experiment, we evaluated virion localization and fluorescence during conditions of direct infection (DI) and SIE. For DI, PRV 137 at an MOI of 100 was applied to uninfected cells. In parallel for SIE, cells were first inoculated with a nonfluorescent PRV followed by application of PRV 137 2 h later. Image acquisition for both conditions began immediately after application of the PRV 137 inoculum and every 2.5 min for a period of 1.5 h.

Representative images at 20-min intervals from the resulting time-lapse movies (Movies S1 and S2 in the supplemental material) are depicted for both DI and SIE. Under conditions of DI (Fig. 3C), we observed separation of fluorescence, with an increased number of red punctate structures within the cell. Capsid internalization and subsequent trafficking toward the nucleus are evidenced by red puncta near the nucleus. In contrast, cells superinfected with PRV 137 (SIE condition) exhibit no internalized or nuclear-associated capsid assemblies (Fig. 3D). In fact, most of the fluorescent structures remain at or near the cellular boundary.
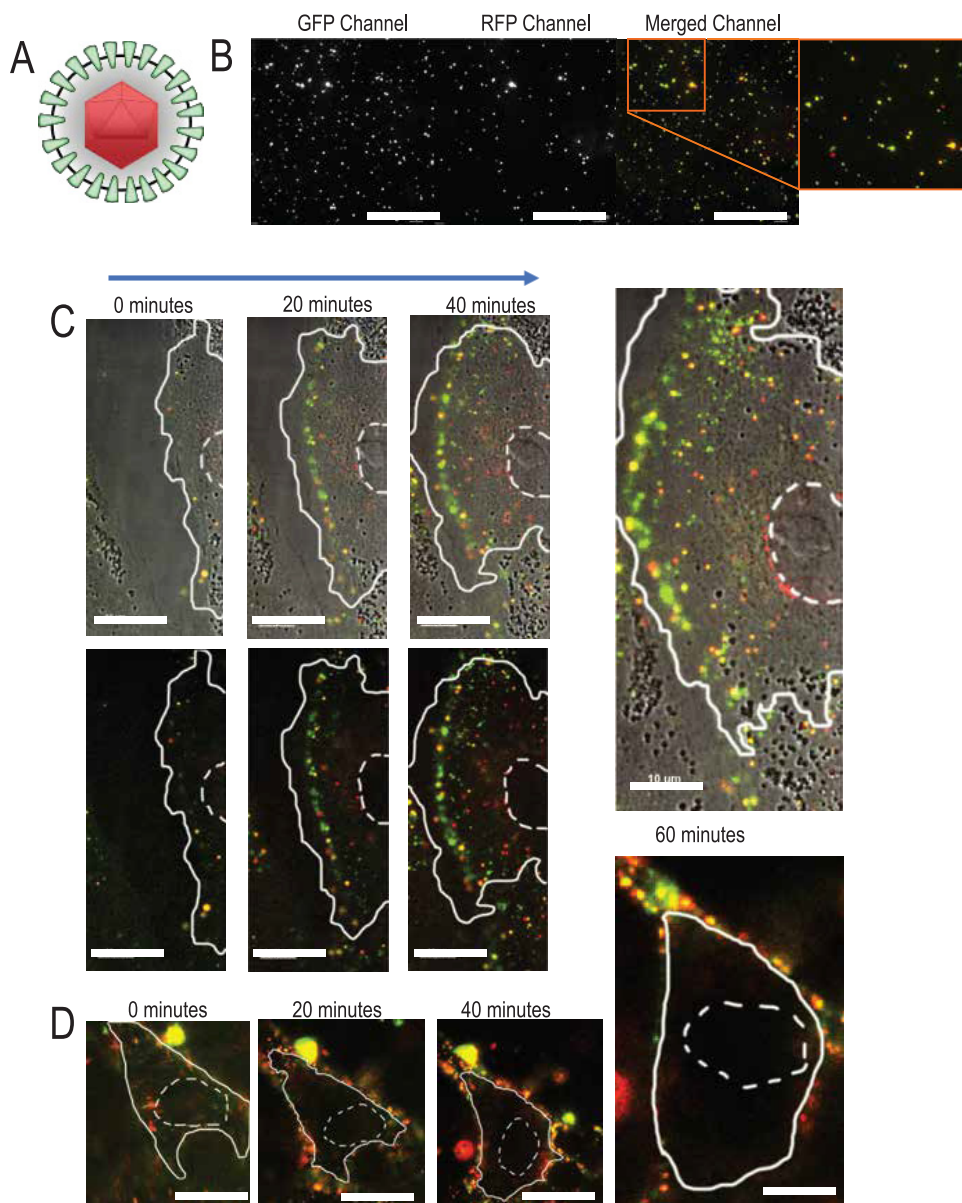
FIG 3 Live fluorescence microscopy observes absence of nuclear localized capsids during SIE. (A) Model of PRV 137 virion containing an mRFP-VP26 fusion (red capsid) and a gM-eGFP fusion (green envelope protein). (B) Distribution of PRV 137 fluorescent assemblies from a viral supernatant preparation. Images are split into designated fluorescent channels and composite image. (C) Select images from a time course of direct infection with PRV 137 on PK15 cells. Images taken every 20 min. The top row corresponds to brightfield and fluorescent composite images, while the bottom row demonstrates only fluorescent merged images. The nucleus is outlined with dashed lines, while the cell boundary is outlined with a solid line. (D) Select images from a time course of PRV 137 during SIE. Images were taken every 20 min after application of PRV 137. Cell boundaries are as depicted above.

These observations are consistent with our expectations that internalization or trafficking of secondary virions is strongly suppressed during SIE. The lack of separation between the two fluorescent labels suggests an impairment of virion fusion, while the absence of internalized red fluorescent capsids is evidence of impaired capsid trafficking. To further evaluate the impact of SIE on secondary virion entry, we sought to develop more quantitative approaches to understand virion trafficking.

SIE in PRV reduces capsid entry. To quantify the extent of virion entry and trafficking, we evaluated the distribution of fluorescent capsids within a 3-dimensional reconstruction of infected cells. Cells were inoculated with mRFP-VP26 labeled capsids (PRV 180 or HSV-1 OK14) under conditions of direct infection, SIE, and SIE with treatment of
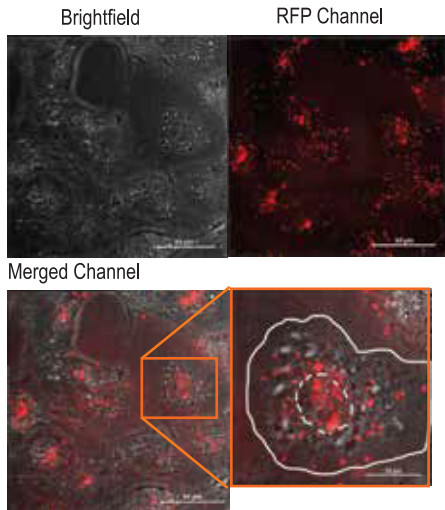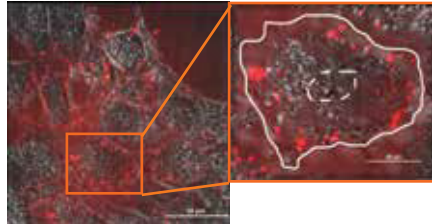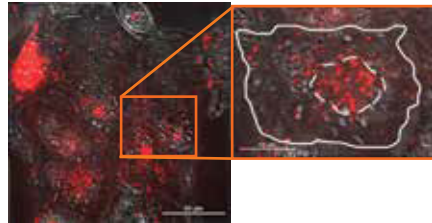
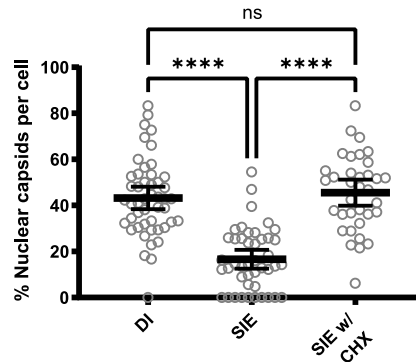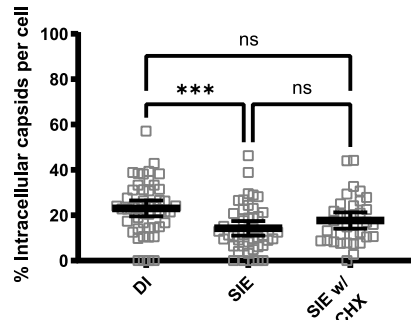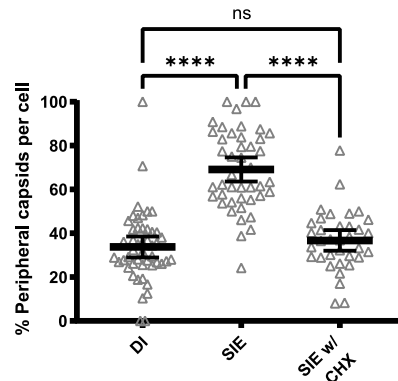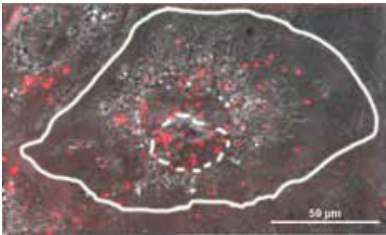**FIG 4** PRV SIE exhibits a strong reduction in nuclear-associated capsids. PK15 cells under indicated conditions. Depicted channels are brightfield, red fluorescence channel, and merged. Inset shows magnified image of a representative single cell from the field. The white dotted line corresponds to the nuclear region of the cell, while a solid line depicts the periphery of the cell. For each condition, a minimum of 3 fields were analyzed and depicted as percentage of total capsids per cell for each category. Quantitative results from single-cell analysis were statistically compared by one-way ANOVA. (A) Direct infection with PRV 180 (MOI 100). (B) SIE infection with primary infection of PRV Becker (MOI 100) and secondary infection of PRV 180. (C) SIE with CHX treatment. CHX treatment occurred between infection of primary and secondary. (D) Dunn's multiple-comparison test (one-way ANOVA) comparing capsid localization between conditions. *, $P = 0.0129$; **, $P = 0.0016$; ***, $P = 0.0004$; ****, $P < 0.0001$.
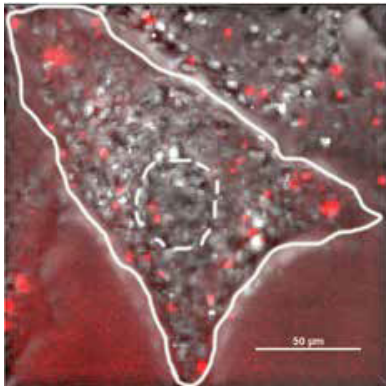
CHX. Following infection, cells were sequentially imaged through their z-axis to acquire a full imaging volume. After image acquisition, cells were rendered into 3D models and individual fluorescent puncta were counted and categorized by relative location in each cell: capsids near the nuclear region (nuclear), within the cellular boundary (intracellular), and at the cellular boundary (peripheral). Analysis of infected cells from each condition excluded cells with extensive fluorescence aggregation or those that contained overlapping cellular boundaries. Representative images of infections under the different conditions are depicted in Fig. 4 to 6.

The counts and categorizations of fluorescent capsid assemblies for PRV are presented in Fig. 4. We were able to quantify an average of 45 virions per cell, with a total of 35 to 48 cells
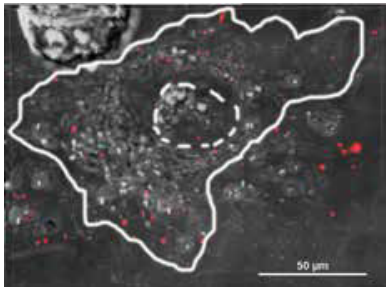
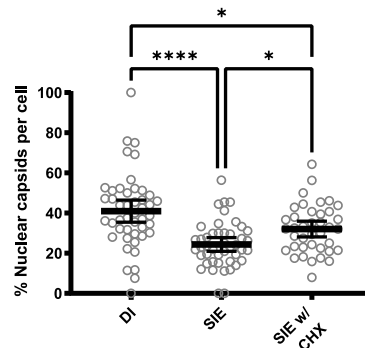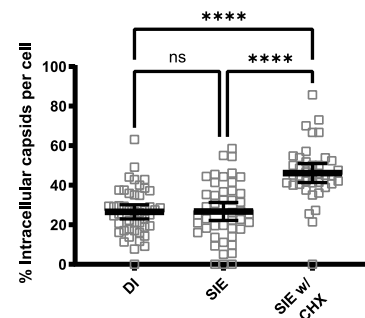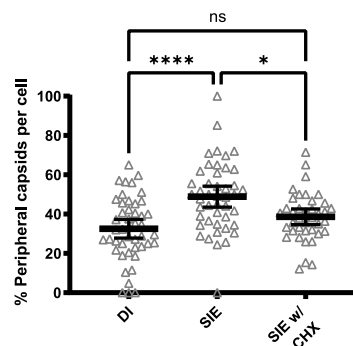**FIG 5** HSV SIE exhibits a modest reduction in nuclear capsids. Representative images of an infected Vero cell with capsid distributions from three conditions of infection. The white dotted line indicates the nuclear region of the cell, while a solid line depicts the periphery of the cell. For each condition, a minimum of 3 fields were analyzed and depicted as percentage of total capsids per cell for each category. Quantitative results from single-cell analysis were statistically compared by one-way ANOVA. (A) Direct infection with HSV OK14 (MOI 100). (B) SIE infection with primary infection of HSV-1 17 (MOI 100) and secondary infection of HSV OK14. (C) SIE with CHX treatment. CHX treatment occurred between infection of primary and secondary. (D) Dunn's multiple-comparison test (on-way ANOVA) comparing capsid localization between conditions. *, $P = 0.0264$; ****, $P < 0.0001$.

within each condition. Plotted are the numbers of capsids categorized for each condition out of the total observed capsids on a per-cell basis. We also compared capsid localization across different conditions to determine the statistical significance between infection conditions.

Comparisons between capsid distributions by condition reveal that there was a strong statistical difference between SIE and direct infection (DI) for all capsid categorizations (Fig. 4A to C). Comparisons of capsid distribution between SIE and DI revealed that there was a significant difference between the nuclear and peripheral distribution of capsids but not any statistical difference for capsids localized to the intracellular region of the cell. For the DI condition, an average of 47% of cell-associated capsids were localized near the nucleus. For the condition of SIE, only 14% of capsids localized near the nucleus. For the condition of SIE with CHX

A **Direct Infection**
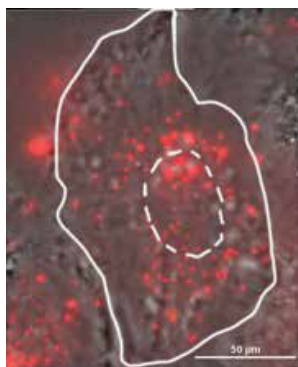
B **SIE**
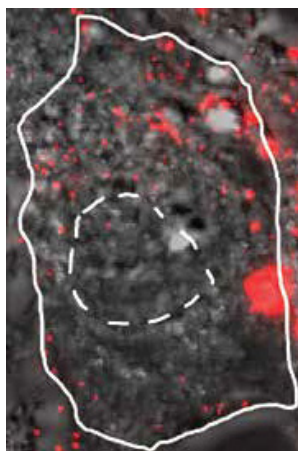
C **SIE w/ CHX**
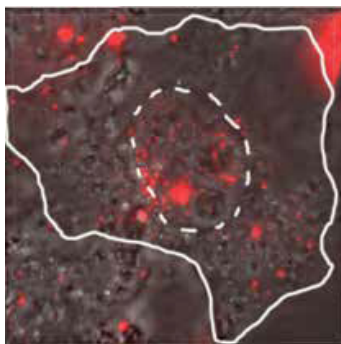
D **gD Null Single-Cell Analysis by Nuclear Capsids**
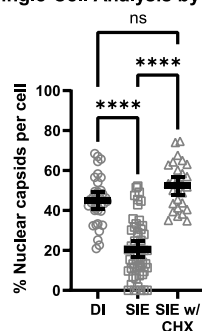
gD Null Single-Cell Analysis by Peripheral Capsids
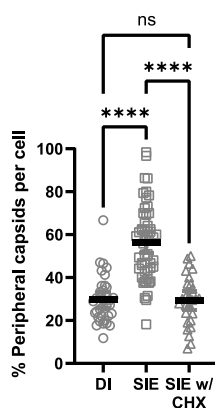
gD Null Single-Cell Analysis by Intracellular Capsids
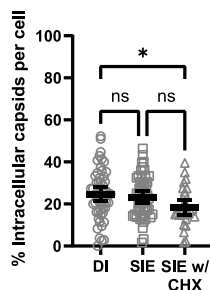
FIG 6 SIE during gD-null infection also reduces nuclear-associated capsids. Representative images of capsid distribution under three conditions of infection. The dotted white line indicates the nuclear region of the cell, while a solid line depicts the periphery of the PK15 cell. For each condition, a minimum of 3 fields were analyzed and depicted as percentage of total capsids per cell for each category. Quantitative results from single-cell analysis were statistically compared by one-way ANOVA. (A) Direct infection with PRV 180 (MOI 100). (B) SIE infection with primary infection of PRV GS442 (gD-null) and secondary infection of PRV 180. (C) SIE infection with CHX treatment. CHX treatment occurred between infection of primary and secondary. (D) Dunn's multiple-comparison test (one-way ANOVA) comparing capsid localization between conditions. *, $P = 0.0292$; ****, $P < 0.0001$.

treatment, capsid distributions more closely matched those of DI conditions, with 47% of capsids at the nucleus. It is important to note that the values are averaged across multiple cells observed for each condition. As a result, most average values underrepresent the most observed state of capsid distribution. For SIE, many cells contain no nuclear capsids, with 100% of capsids retained at the periphery. The overall reduction of nuclear capsids and the accumulation of peripheral capsids during SIE correlate with our live fluorescence microscopy

observations. Together, the difference in capsid distribution is consistent with our prior interpretation that PRV-induced SIE inhibits secondary virion entry.

HSV-1 SIE does not alter intracellular capsid accumulation. To compare how SIE alters secondary capsid uptake between different alphaherpesviruses, we performed a parallel experiment with HSV-1 expressing an mRFP fusion to VP26 (HSV-1 OK14) under similar conditions. We quantified an average of 40 capsids per cell, analyzing between 39 and 46 cells per condition.

Results from the quantification of mRFP-labeled HSV-1 capsids revealed a surprising difference of capsid distribution compared to that of PRV. As shown in Fig. 5D, there was a reduction of nuclear capsids and an increase in peripheral capsids between HSV SIE and HSV DI. However, most cells in the SIE condition did have detectable capsids localized to the nuclear boundary. This differs from PRV, where most cells under SIE lacked any nuclear localized capsids. Moreover, treatment with CHX in HSV-1 SIE elicited a strong increase in intracellular capsids but did fully match distributions seen for DI conditions. These differences in capsid distribution seem to indicate that HSV does not interfere with superinfecting virion entry to the same extent as PRV.

PRV gD expression is not necessary to reduce capsid trafficking. We previously determined that SIE for PRV occurred independently of gD expression (4). However, it does not eliminate the possibility that gD expression could be interfering with the entry of the superinfecting virion. To test if gD expression is necessary for the observed reduction in capsid entry during PRV SIE, a gD-null virus (PRV GS442) was utilized as a primary inoculum.

Using the conditions already defined in Fig. 4, an average number of 58 fluorescent capsids were quantified for 30 to 55 cells for each condition. Although this is a greater average count per cell than that of the prior analyses, aggregates of fluorescent capsids were more extensive during superinfection of gD-null infected cells. Cells with excessive capsid aggregation were excluded from quantification with our analysis focusing on cells with individual capsid assemblies.

SIE following gD-null primary inoculation was very similar to our previous observation of decreased capsid association with the nucleus and accumulation of capsids at the periphery (Fig. 6). Comparing the capsid distributions demonstrated a significant reduction (approximately 50%) for nuclear internalization between DI and SIE with no difference between DI and SIE with CHX treatment. There is an increase of capsids on the periphery of the cell for SIE only with no differences between DI and SIE with CHX treatment. The only distinct difference between wild-type SIE and gD-null SIE is the percentage of intracellular capsids not associated with the nucleus. This lack of difference in internalized capsids may be related to the accumulation of fluorescent capsid assemblies at the periphery or to changes in secondary virion fusion compared to that of wild-type PRV primary infection. Despite the subtle changes in capsid uptake, the reduction in nuclear capsid association following gD-null primary infection is consistent with a mechanism inhibiting virion entry that is independent of gD expression.

DISCUSSION

This study probed the effect of glycoprotein D-independent SIE during secondary entry of the alphaherpesviruses PRV and HSV-1. We observed that the MOI for both the primary and secondary inocula played a significant role in the establishment and extent of exclusion. A higher-MOI secondary inoculum was able to overcome SIE, while lower MOIs of secondary challenge are more efficiently excluded. One possible explanation for these observations is that higher-MOI primary infections exhibit expedited viral gene expression and implementation of SIE. For example, an MOI of 10 for the initial virus completely failed to exclude a superinfecting MOI of 25, while an initial MOI of 25 required a superinfecting MOI of 100 to achieve a similar expression of SIE. Additionally, conditions with a higher initial MOI are more capable of excluding the secondary virus (as shown in the columns when comparing conditions like MOI 50 and 100 with a lower secondary viral infection). Our experiments have demonstrated that infection of the primary virus was extensive (as shown through CFP expression), indicating that the observable phenomenon is not misrepresented by lack of infection of the primary virus. This suggests that the kinetics of viral replication

and genome production likely play roles in regulating implementation of SIE. The importance of primary viral genome number and subsequent protein production was further confirmed using CHX to inhibit protein production by the primary viral infection. High or low inoculation with similar MOIs and CHX treatment alleviated SIE. This indicates that it is not just the presence of a high inoculating virus but also its amount relative to that of the secondary virus.

Although concurrent results indicate viral factors can influence the extent of SIE, nonviral factors could not be excluded. To this end, we evaluated surface expression of nectin-1 during infection. Although there is a drop in nectin-1 following initial infection at 0 h postinfection, the level of surface nectin-1 is similar when treated with CHX. Since CHX has previously been shown to alleviate SIE, the limited nectin-1 present on the surface is still capable of mediating superinfection. This observation strongly suggests that interference with cell surface presentation of entry receptors is not important for the mechanism of alphaherpesvirus SIE.

To identify the step of viral infection affected by gD-independent SIE, we visualized capsid entry with live fluorescence microscopy. Dual-labeled virions allowed the observation of distinct fluorescent profiles for virion distribution between SIE and direct infection conditions. Accumulation of dual fluorescent PRV virions at the plasma membrane of cells during SIE suggests an inhibition of virion fusion and confirms prevention of entry. This is further supported by the quantitative analysis of fluorescent capsids, which revealed strong reductions in nuclear association following entry. These results raise the possibility that gD-independent SIE might inhibit virion entry or subsequent trafficking.

Initially, it was expected that the effect of SIE on entry would be similar between alphaherpesviruses due to observations of SIE for HSV-1 and PRV in Criddle et al. (23). Although the outcome of SIE suppression remains similar across alphaherpesviruses, experiments from this paper demonstrated that the mechanisms of how HSV-1 and PRV SIE operate may differ. PRV-mediated SIE results in reduced capsid internalization, with most accumulating on the periphery. This could be a result in which the PRV mechanism of SIE inhibits both direct fusion and low endocytic processes, allowing the strong accumulation of virions on the surface of the cell. HSV-1 SIE, however, does not exhibit reduced capsid internalization while still resulting in accumulation on the periphery. This result indicates that HSV-1 SIE might employ a combination of postentry factors to suppress expression of a superinfecting virus, while PRV SIE likely targets only virion fusion (Fig. 7). This difference strongly suggests that there are multiple mechanisms employed by alphaherpesviruses to suppress superinfection. The single-cell analysis of capsid distribution is one potential means for continued study into the differences of SIE between related viruses.

Taken together, work from this study provides new insights into the properties of alphaherpesvirus SIE. This work supports our previous finding that SIE is a virally induced, gD-independent phenotype but differs in the mechanism of exclusion between PRV and HSV-1. PRV-mediated SIE appears to inhibit entry of secondary virions in a gD-independent manner, while HSV-1 SIE affects a postentry step. Further work will further characterize the differences between PRV and HSV-1 SIE, as well as identify the viral mechanism(s) which mediate exclusion. Most likely, this will address the kinetics of viral protein between primary and secondary challenge of viruses. These data about gD-independent SIE will provide valuable insight regarding alphaherpesvirus population dynamics, disease kinetics for neuronal pathologies, and development of antiviral therapies.

MATERIALS AND METHODS

Cells and viruses. Porcine kidney epithelial cells (PK15), G5 cells, and green African monkey kidney (Vero) cell lines were obtained from the Enquist laboratory. Human keratinocyte cells (HaCat) were obtained from ATCC. All cells were maintained in Dulbecco's modified Eagle's medium (DMEM) supplemented with 10% (vol/vol) fetal bovine serum (FBS) and 1% (vol/vol) penicillin-streptomycin. PRV stocks and plaque assays were performed on PK15 cells as described previously (37). PRV isolates containing glycoprotein D deletion were propagated on PK15 cells that stably express glycoprotein D (G5 cells) needed for supporting virion infectivity (23, 38, 39). These cells were cultured as described above but supplemented with histidinol (50 μg/mL) to maintain glycoprotein D expression. HSV stocks were propagated and the titers determined on Vero cells (40).

All fluorescent PRV recombinants were derived from a PRV Becker background. PRV 287 and 289 express either an enhanced yellow fluorescent protein (eYFP) or a cyan fluorescent protein (Turq2) fused to a 3×NLS signal peptide as described previously (23, 40). PRV 180 contains an mRFP fusion to the
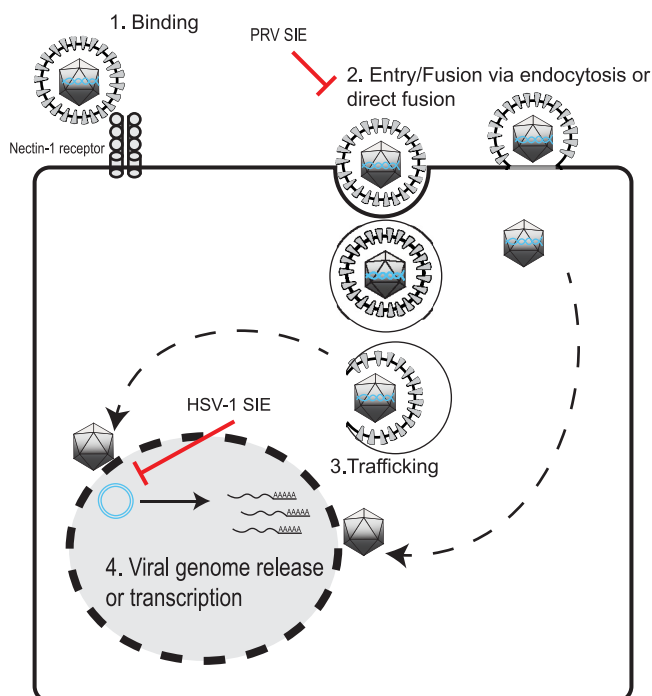
FIG 7 Model of SIE inhibition of alphaherpesviruses. A schematic representation of the proposed points of inhibition of secondary virion infection during SIE. PRV SIE suppresses entry/fusion, while HSV-1 possibly inhibits viral genome release or transcription.

minor capsid protein VP26 as characterized previously (41). PRV 137 expresses both an eGFP in-frame fusion to gM and an mRFP fusion to VP26 as described previously (36). PRV GS442 was a kind gift from Greg Smith and the Enquist Lab. PRV GS442 is a viral mutant lacking glycoprotein D expression. A PRV bacterial artificial chromosome (BAC) was utilized to excise the gD gene via homologous recombination inserting a diffusible green fluorescent protein (eGFP). Originally, stocks of PRV GS442 were maintained in a mixture of G5 and PK15 cells in a ratio of approximately 3:1. Viral titers of PRV GS442 were determined with PK15 cells (23, 38, 39). Fluorescent HSV-1 recombinants were derived from HSV-1 strain 17. HSV-1 OK14 expresses an mRFP fusion to the capsid protein VP26 (41).

All stocks of fluorescent viruses were confirmed by fluorescence microscopy of plaques to ensure maintenance and fidelity of the associated fluorescent profiles. Experiments requiring fluorescent virions utilized fresh viral supernatants. Stocks were initiated with an MOI 10 infection of a 10-cm dish of support cells. At 24 h postinfection, the medium was collected and subjected to low-speed centrifugation to remove cells and debris. The medium was supplemented with 20 mM HEPES (pH 7.0). Cell-free viral stocks of PRV 180 and HSV-1 OK14 were stored in 500-μL aliquots to maximize virion-associated fluorescence.

Microscopy. Images were acquired on a Nikon Ti-Eclipse (Nikon Instruments, Melville, NY) inverted microscope equipped with a SpectraX LED (Lumencor, Beaverton, OR) excitation module and fast-switching emission filter wheels (Prior Scientific, Rockland, MA). Fluorescence imaging used paired excitation/emission filters and dichroic mirrors for cyan fluorescent protein (CFP), YFP, and RFP (Chroma Technology Corp., Bellow Falls, VT). Brightfield images utilized a Plan Fluor 20 phase contrast (Ph) objective and an iXon 896 EM-CCD (Andor Technology Ltd., Belfast, Northern Ireland) camera using NIS-Elements software. Acquisition of fluorescent virions utilized a CFI Plan Apochromat Lambda 60$\times$ and 100$\times$ oil immersion objective to visualize individual virion localization within infected cells. Infected cells were imaged at the time postinfection indicated in each figure legend, dependent on experimental design. Experiments were tested at least twice with multiple fields acquired for each condition of the experiment.

Live imaging was performed on the microscope in conjunction with a stage-top incubation system (Quorum Scientific, Puslinch, Ontario, Canada). PK15 cells were cultured on Lab-Tek II chambered coverglass. Prior to imaging, a nonfluorescent primary virus was used to establish primary infection, washed, and then fed with medium for 2 h before the secondary infection was applied. Cells were maintained at 37°C in a 5% (vol/vol) CO_2-enriched atmosphere using a stage-top incubator system. Imaging began directly after application of fluorescent viral inoculum, as described. Images were acquired every 2.5 min, and fluorescent illumination intensity was set to 35% power with less than 100 ms exposure for each channel to avoid photobleaching.

Flow cytometry. Detection of extracellular nectin-1 in infected cells was performed using a BD LSR II or BD LSR Fortessa cytometer (BD Biosciences, San Jose, CA). Infected cells were harvested by 5 mM EDTA supplemented with Dulbecco's phosphate-buffered saline (D-PBS) and washed once with Ca^{2+}- and Mg^{2+}-free D-PBS with 0.1% bovine serum albumin (BSA; flow cytometry buffer). Cells were then fixed with 2% paraformaldehyde (PFA), washed with 1$\times$ PBS solution, and resuspended in 200 μL of flow cytometry buffer. Fixed cells were incubated with mouse IgG monoclonal nectin-1-specific antibody (CK8) (ThermoFisher, Waltham, MA) at 2.5 μg/mL for 1 h at room temperature. Cells were washed again and subsequently incubated with secondary

goat anti-mouse IgG conjugated to Alexa Fluor 488 (ThermoFisher, Waltham, MA). After 1 h of incubation, cells were washed with 1× PBS solution and resuspended in flow cytometry buffer for analysis. Acquisition and gating were set on mock-infected and nonspecific, secondary antibody-stained infected cell populations. All cytometry data were analyzed using the FlowJo data analysis software (FlowJo, LLC, Ashland, OR).

MOI dependency for superinfected cells. FP expression in infected cells was assessed through fluorescence microscopy. The day before experiments, 1.0×10^5 PK15 cells per well were seeded in 12-well plates. The next day, at time T = −1 h, initial inoculations across four MOI conditions (10, 25, 50, and 100) were performed with PRV 289. One hour postinoculation, inoculum was aspirated, and cells were washed with 2 mL PBS per well. Then, 1 mL of viral medium (DMEM, 2% FBS, 1% Pen-Strep) was supplemented into each well. This time point, T = 0 h, was taken to be the time of initial infection. At T = 2 h, medium was aspirated, cells were again washed with 2 mL PBS per well, and secondary inoculations were performed with PRV 287. These infections were also performed across four MOI conditions (10, 25, 50, and 100), such that a 4 by 4 matrix was generated whereby every initial infection condition was subjected to every superinfection condition. At T = 3 h, superinfecting inoculum was aspirated, cells were washed with PBS, and cells were again overlaid with 1 mL viral medium per well. Finally, at T = 6 h, cells were imaged on brightfield, CFP, and YFP channels using paired fluorescent filters. In certain experiments, cycloheximide (CHX) was used to inhibit protein synthesis in the initial inoculation. In these cases, after the wash of the initial inoculum at T = 0, cells were overlaid with 1 mL viral medium per well supplemented with 100 μg/mL cycloheximide (CHX). Consequently, at T = 2 h, cells were subjected to two washes with PBS prior to application of the second inoculum to ensure removal of any CHX during subsequent incubations.

Virion localization. Fluorescent virion assemblies were imaged on an epifluorescence microscope and photomicrographs were acquired with 60× and ×100 magnification objectives. Sequential photos of infected cells through the z-axis (z-stacks) were acquired and used to generate a 3D reconstruction with NIS-Elements software to facilitate analysis of capsid localization on a per-cell basis. Individual capsid assemblies were then counted in a single-cell analysis based upon their localization in the cell: perinuclear virions (adjacent to nuclear region of cell), intracellular virions (inside cellular membrane), and external virions (virions attached but unentered). Average counts of virions were then compared across all conditions and represented out of total virions.

The following conditions were used for experimental procedures: direct infection (DI), SIE, and SIE with CHX. Direct infections were established by the inoculation of mRFP-VP26 virions (HSV-1 OK14 and PRV 180) onto Vero or PK15 cells, respectively, for a 1-h duration in a 37°C incubator. For SIE, cells were initially inoculated for 1 h at 37°C with a nonfluorescent HSV-1 or PRV wild-type virus. Cells were then washed and maintained for 3 h at 37°C. Afterward, they were subsequently infected with mRFP-VP26-labeled virions as described for direct infection. For SIE with CHX, cells were initially inoculated for 1 h at 37°C with a nonfluorescent HSV-1 or PRV wild-type virus and then washed and supplemented with medium containing CHX at 100 μg/mL during the 3-h incubation at 37°C. After incubation, cells were subsequently infected with mRFP-VP26-labeled virions as described for direct infection. One hour after application of fluorescent virions, cells were washed and supplemented with fresh cellular medium.

Statistical analysis of virion localization. To compare the statistical differences between conditions of the virion localization experiments, statistical analysis was performed through GraphPad Prism (GraphPad Software, San Diego, CA, USA). To process the data derived from capsid localization, descriptive statistics was used in Prism to determine basic statistical parameters of quartiles, mean, and 95% confidence interval. D'Agostino and Pearson tests were applied to confirm that the data sets did not follow parameters of normal standardization due to the presence of outliers. Statistical comparisons were done with Kruskal Wallis tests and with Dunn's multiple-comparison test as a means for comparing differences between conditions (SIE, DI, and SIE with CHX). One-way analysis of variance (ANOVA) graphs depicting statistical significance and single-cell analysis comparing the localization of viral capsids among conditions are shown in Fig. 4 to 6.

SUPPLEMENTAL MATERIAL

Supplemental material is available online only.
SUPPLEMENTAL FILE 1, AVI file, 7.9 MB.
SUPPLEMENTAL FILE 2, AVI file, 7.1 MB.

ACKNOWLEDGMENTS

REFERENCES

1. Loncoman CA, Vaz PK, Coppo MJ, Hartley CA, Morera FJ, Browning GF, Devlin JM. 2017. Natural recombination in alphaherpesviruses: insights into viral evolution through full genome sequencing and sequence analysis. Infect Genet Evol 49:174–185. https://doi.org/10.1016/j.meegid.2016.12.022.
2. Looker KJ, Magaret AS, May MT, Turner KME, Vickerman P, Gottlieb SL, Newman LM. 2015. Global and regional estimates of prevalent and incident herpes simplex virus type 1 infections in 2012. PLoS One 10:e0140765. https://doi.org/10.1371/journal.pone.0140765.
3. Mertz GJ. 2008. Asymptomatic shedding of herpes simplex virus 1 and 2: implications for prevention of transmission. J Infect Dis 198:1098–1100. https://doi.org/10.1086/591914.
4. Rooney BV, Crucian BE, Pierson DL, Laudenslager ML, Mehta SK. 2019. Herpes virus reactivation in astronauts during spaceflight and its application on earth. Front Microbiol 10:16. https://doi.org/10.3389/fmicb.2019.00016.
5. Casto AM, Roychoudhury P, Xie H, Selke S, Perchetti GA, Wofford H, Huang M-L, Verjans GMGM, Gottlieb GS, Wald A, Jerome KR, Koelle DM, Johnston C,

Greninger AL. 2020. Large, stable, contemporary interspecies recombination events in circulating human herpes simplex viruses. J Infect Dis 221:1271–1279. https://doi.org/10.1093/infdis/jiz199.

6. Bowden R, Sakaoka H, Donnelly P, Ward R. 2004. High recombination rate in herpes simplex virus type 1 natural populations suggests significant co-infection. Infect Genet Evol 4:115–123. https://doi.org/10.1016/j.meegid.2004.01.009.

7. Schmid DS. 2019. Mixing it up: new insights into interspecies recombination between herpes simplex virus type 1 and 2. J Infect Dis 18:1208–1209. https://doi.org/10.1093/infdis/jiz200.

8. Bowen CD, Renner DW, Shreve JT, Tafuri Y, Payne KM, Dix RD, Kinchington PR, Gatherer D, Szpara ML. 2016. Viral forensic genomics reveals the relatedness of classic herpes simplex virus strains KOS, KOS63, and KOS79. Virology 492:179–186. https://doi.org/10.1016/j.virol.2016.02.013.

9. Song R, Koyuncu OO, Greco TM, Diner BA, Cristea IM, Enquist LW. 2016. Two modes of the axonal interferon response limit alphaherpesvirus neuroinvasion. mBio 7:2145-15. https://doi.org/10.1128/mBio.02145-15.

10. Koelle DM, Norberg P, Fitzgibbon MP, Russell RM, Greninger AL, Huang M-L, Stensland L, Jing L, Magaret AS, Diem K, Selke S, Xie H, Celum C, Lingappa JR, Jerome KR, Wald A, Johnston C. 2017. Worldwide circulation of HSV-2 × HSV-1 recombinant strains. Sci Rep 7:44084. https://doi.org/10.1038/srep44084.

11. Meurens F, Schynts F, Keil GM, Muylkens B, Vanderplasschen A, Gallego P, Thiry E. 2004. Superinfection prevents recombination of the alphaherpesvirus bovine herpesvirus 1. J Virol 78:3872–3879. https://doi.org/10.1128/jvi.78.8.3872-3879.2004.

12. Dasika GK, Letchworth GJ. 2000. Homologous and heterologous interference requires bovine herpesvirus-1 glycoprotein D at the cell surface during virus entry. J Gen Virol 81:1041–1049. https://doi.org/10.1099/0022-1317-81-4-1041.

13. Sloutskin A, Yee ME, Kinchington PR, Goldstein RS. 2014. Varicella-zoster virus and herpes simplex virus 1 can infect and replicate in the same neurons whether co- or superinfected. J Virol 88:5079–5086. https://doi.org/10.1128/JVI.00252-14.

14. Casto AM, Huang M-LW, Xie H, Jerome KR, Wald A, Johnston CM, Greninger AL. 2020. Herpes simplex virus mistyping due to HSV-1 × HSV-2 interspecies recombination in viral gene encoding glycoprotein B. Viruses 12:860. https://doi.org/10.3390/v12080860.

15. Bo Z, Miao Y, Xi R, Gao X, Miao D, Chen H, Jung Y-S, Qian Y, Dai J. 2021. Emergence of a novel pathogenic recombinant virus from Bartha vaccine and variant pseudorabies virus in China. Transbound Emerg Dis 68:1454–1464. https://doi.org/10.1111/tbed.13813.

16. McKinney HH. 1926. Virus mixtures that may not be detected in young tobacco plants. Phytopathology 16:89.

17. Matthews REF. 2002. "Chapter 17." Plant Virology, 4th Edn. Academic Press, New York, 6584582.

18. Jolicoeur P. 1979. The Fv-1 gene of the mouse and its control of murine leukemia virus replication. Curr Top Microbiol Immunol, 86:67–122. https://doi.org/10.1007/978-3-642-67341-2_3.

19. Huang I-C, Li W, Sui J, Marasco W, Choe H, Farzan M. 2008. Influenza A virus neuraminidase limits viral superinfection. J Virol 82:4834–4843. https://doi.org/10.1128/JVI.00079-08.

20. Michel N, Allespach I, Venzke S, Fackler OT, Keppler OT. 2005. The nef protein of human immunodeficiency virus establishes superinfection immunity by a dual strategy to downregulate cell-surface CCR5 and CD4. Curr Biol 15:714–723. https://doi.org/10.1016/j.cub.2005.02.058.

21. Walters K-A, Joyce MA, Addison WR, Fischer KP, Tyrrell DLJ. 2004. Superinfection exclusion in duck hepatitis B virus infection is mediated by the large surface antigen. J Virol 78:7925–7937. https://doi.org/10.1128/JVI.78.15.7925-7937.2004.

22. Geib T, Sauder C, Venturelli S, Hässler C, Staeheli P, Schwemmle M. 2003. Selective virus resistance conferred by expression of borna disease virus nucleocapsid components. J Virol 77:4283–4290. https://doi.org/10.1128/JVI.77.7.4283-4290.2003.

23. Criddle A, Thornburg T, Kochetkova I, DePartee M, Taylor MP. 2016. gD-independent superinfection exclusion of alphaherpesviruses. J Virol 90:4049–4058. https://doi.org/10.1128/JVI.00089-16.

24. Centifanto-Fitzgerald YM, Varnell ED, Kaufman HE. 1982. Initial herpes simplex virus type 1 infection prevents ganglionic superinfection by other strains. Infect Immun 35:1125–1132. https://doi.org/10.1128/iai.35.3.1125-1132.1982.

25. Fuller AO, Spear PG. 1987. Anti-glycoprotein D antibodies that permit adsorption but block infection by herpes simplex virus 1 prevent virion-cell fusion at the cell surface. Proc Natl Acad Sci U S A 84:5454–5458. https://doi.org/10.1073/pnas.84.15.5454.

26. Linehan MM, Richman S, Krummenacher C, Eisenberg RJ, Cohen GH, Iwasaki A. 2004. In vivo role of nectin-1 in entry of herpes simplex virus type 1 (HSV-1) and HSV-2 through the vaginal mucosa. J Virol 78:2530–2536. https://doi.org/10.1128/jvi.78.5.2530-2536.2004.

27. Akhtar J, Tiwari V, Oh M-J, Kovacs M, Jani A, Kovacs SK, Valyi-Nagy T, Shukla D. 2008. HVEM and nectin-1 are the major mediators of herpes simplex virus 1 (HSV-1) entry into human conjunctival epithelium. Invest Ophthalmol Vis Sci 49:4026–4035. https://doi.org/10.1167/iovs.08-1807.

28. Folimonova SY. 2012. Superinfection exclusion is an active virus-controlled function that requires a specific viral protein. J Virol 86:5554–5561. https://doi.org/10.1128/JVI.00310-12.

29. Tebaldi G, Pritchard SM, Nicola AV. 2020. Herpes simplex virus entry by a nonconventional endocytic pathway. J Virol 94:e01910-20. https://doi.org/10.1128/JVI.01910-20.

30. Spear PG. 2004. Herpes simplex virus: receptors and ligands for cell entry. Cell Microbiol 6:401–410. https://doi.org/10.1111/j.1462-5822.2004.00389.x.

31. Nagel CH, Döhner K, Binz A, Bauerfeind R, Sodeik B. 2012. Improper tagging of the non-essential small capsid protein VP26 impairs nuclear capsid egress of herpes simplex virus. PLoS One 7:e44177. https://doi.org/10.1371/journal.pone.0044177.

32. Deschamps T, Dogrammatzis C, Mullick R, Kalamvoki M. 2017. Cbl E3 ligase mediates the removal of nectin-1 from the surface of herpes simplex virus 1-infected cells. J Virol 91:e00393-17. https://doi.org/10.1128/JVI.00393-17.

33. Stiles KM, Krummenacher C. 2010. Glycoprotein D actively induces rapid internalization of two nectin-1 isoforms during herpes simplex virus entry. Virology 399:109–119. https://doi.org/10.1016/j.virol.2009.12.034.

34. Geraghty RJ, Jogger CR, Spear PG. 2000. Cellular expression of alphaherpesvirus gD interferes with entry of homologous and heterologous alphaherpesviruses by blocking access to a shared gD receptor. Virology 268:147–158. https://doi.org/10.1006/viro.1999.0157.

35. Jarosinski KW. 2012. Dual infection and superinfection inhibition of epithelial skin cells by two alphaherpesviruses co-occur in the natural host. PLoS One 7:e37428. https://doi.org/10.1371/journal.pone.0037428.

36. Hogue IB, Bosse JB, Hu JR, Thiberge SY, Enquist LW. 2014. Cellular mechanisms of alpha herpesvirus egress: live cell fluorescence microscopy of pseudorabies virus exocytosis. PLoS Pathog 10:e1004535. https://doi.org/10.1371/journal.ppat.1004535.

37. del Rio T, Werner HC, Enquist LW. 2002. The pseudorabies virus VP22 homologue (UL49) is dispensable for virus growth in vitro and has no effect on virulence and neuronal spread in rodents. J Virol 76. https://doi.org/10.1128/JVI.76.2.774-782.2002.

38. Campadelli-Fiume G, Qi S, Avitabile E, Foà-Tomasi L, Brandimarti R, Roizman B. 1990. Glycoprotein D of herpes simplex virus encodes a domain which precludes penetration of cells expressing the glycoprotein by superinfecting herpes simplex virus. J Virol 64. https://doi.org/10.1128/JVI.64.12.6070-6079.1990.

39. Smith GA, Enquist LW. 2000. A self-recombining bacterial artificial chromosome and its application for analysis of herpesvirus pathogenesis. Proc Natl Acad Sci U S A 97:4873–4878. https://doi.org/10.1073/pnas.080502497.

40. Huber MT, Wisner TW, Hegde NR, Goldsmith KA, Rauch DA, Roller RJ, Krummenacher C, Eisenberg RJ, Cohen GH, Johnson DC. 2001. Herpes simplex virus with highly reduced gD levels can efficiently enter and spread between human keratinocytes. J Virol 75.

41. del Rio T, Ch'ng TH, Flood EA, Gross SP, Enquist LW. 2005. Heterogeneity of a fluorescent tegument component in single pseudorabies virus virions and enveloped axonal assemblies. J Virol 79:3903–3919. https://doi.org/10.1128/JVI.79.7.3903-3919.2005.